Thermal Analysis and Topographical Characterization of Films of Styrene-Butadiene Blends

Petri Ihalainen,[1] Kaj Backfolk,[2] Petri Sirviö,[2] Jouko Peltonen[3]

[1]*Center for Functional Materials, Department of Physical Chemistry, Åbo Akademi University, Porthaninkatu 3-5, FI-20500 Turku, Finland*
[2]*Stora Enso Oyj, Imatra Research Center, FI-55 800 Imatra, Finland*
[3]*Center for Functional Materials, Laboratory of Paper Coating and Converting, Åbo Akademi University, Porthaninkatu 3-5, FI-20500 Turku, Finland*

Received 5 July 2007; accepted 20 December 2007
DOI 10.1002/app.28115
Published online 28 March 2008 in Wiley InterScience (www.interscience.wiley.com).

ABSTRACT: Scanning probe microscopy (SPM) was used to study the thermal characteristics of latex films consisting of blends of two different styrene-butadiene copolymers with different glass transition temperatures (T_g). The resonance frequency (ω) and the quality factor (Q_p) of an SPM probe oscillating above the sample surface were determined at different probe temperatures (T_p). Thermal transitions associated with a change in heat capacity were observed in the $\Delta\omega$-T_p curves. The results were compared with differential scanning calorimetry measurements. The very slow heating rate used in the SPM method effectively eliminated the contribution of volumetric changes of the films around T_g. Annealing of the samples in an oven did not influence the thermal transitions observed in the $\Delta\omega$-T_p curves. The SPM method also enabled a novel approach for determining transition-induced dimensional changes (vertical contraction, expansion) of the films. Annealing was found to increase the dimensional stability of the blend films. The latex blends were also annealed by the SPM probe and the film progressed from particulate phase morphology to a continuous phase. © 2008 Wiley Periodicals, Inc. J Appl Polym Sci 109: 322–332, 2008

Key words: polymer blend films; scanning probe microscopy; thermal properties; heat capacity; dimensional stability

INTRODUCTION

An increasing number of technological applications for polymer films have increased the need to study their mechanical, thermal, and surface properties. The development of reactive blends, polyolefin blends, glassy polymer-elastomer blends, and emulsion blends from relatively inexpensive components is today the method of preference in polymer industry.[1]

Of special technological and scientific interest are simple latex emulsion blends of film-forming (low-T_g or ''soft'') and nonfilm-forming (high-T_g or ''hard'') components.[2–24] From a technological point of view, the use of soft/hard latex blends offers an effective strategy for removing environmentally harmful volatile organic compounds from water-borne coating formulations. They also provide means of achieving water-borne coatings with good film-forming properties and good blocking resistance as well as sufficient mechanical strength and durability at the application temperatures. Hard latex particles provide the necessary blocking resistance and mechanical strength and integrity to the film, while soft latex particles act as film-forming components. Properties such as interfacial compatibility between hard and soft constituents, particle size and size ratio of components, and the blend composition need to be optimized to obtain a homogeneous blend with good film-forming characteristics and mechanical properties.

Several mechanical and thermal methods are available for determining the bulk or surface T_g and the overall thermal properties of polymers and polymer blends. The most common bulk methods include differential scanning calorimetry (DSC), differential thermal scanning analysis, dynamical mechanical analysis, dynamical mechanical thermal analysis, and thermo mechanical analysis (TMA).[25] Various modes of scanning probe microscopy (SPM) have been used to study thermal properties of polymer films, including hot-stage and scanning thermal microscopy,[26–39] friction (lateral) force microscopy,[40–42] shear-modulated scanning force microscopy,[43,44] force-distance measurements,[45] scanning local acceleration microscopy,[46] and detection of the resonance frequency of an SPM probe oscillating just above a heated sample.[47–50]

Recently, the SPM probe was utilized simultaneously as a thermal actuator (heater) and a sensor for

Correspondence to: J. Peltonen (jouko.peltonen@abo.fi).
Contract grant sponsor: Finnish Funding Agency for Technology and Innovation (Tekes).

detecting thermal transitions in styrene-butadiene copolymer latex films[51,52] and polyester and styrene/acrylate composite powders.[53] The resonance frequency (ω) of a heated probe oscillating above the sample surface was determined at different probe temperatures (T_p). The transitions seen in the $\Delta\omega$-T_p curves were interpreted as being due to changes in heat capacity of the studied films.[51] The heating-by-the-probe method was observed to cause local, controlled annealing of the polymer film surface. The heating rate in this system is very slow; for example, the contribution of volumetric changes around T_g involved in DSC measurements is effectively eliminated in this SPM heating method.

In the present study, we have used the SPM heating-by-the-probe method to detect thermal transitions in films of emulsion blends. Special attention was paid to sample annealing history. Furthermore, a novel approach for detecting dimensional changes associated with thermal transitions is introduced. This SPM probe quality factor response method involves determining the quality factor of the probe (Q_p) at different probe temperatures, T_p. The sign of ΔQ_p indicates whether the sample is contracting or expanding vertically. The heat-induced topographical changes and film formation of the latex blend films during the SPM probe annealing were also studied. A set of roughness parameters calculated from the SPM image data were used to quantify the essential features of the film surfaces.

MATERIALS AND METHODS

Sample preparation

Two styrene-butadiene copolymer latex samples were provided as aqueous emulsions by Omnova Solution (USA). Latex A was a mixture of styrene (82.6 wt %) and butadiene (15.0 wt %), and Latex B was a mixture of styrene (92.8 wt %) and butadiene (5.0 wt %). Latex A represents a low-T_g component and Latex B a high-T_g component. Latex B was more crosslinked than Latex A; the gel content for Latex A was 25 wt % and for Latex B 62%. Both emulsions included an alkyl diphenylene oxide sulfonate surfactant (2 wt %) and were acidified with acrylic acid. The dry solids contents of both the copolymer emulsions were $\sim$ 50 wt %. The average particle sizes of the Latex A and Latex B emulsions were 180 and 160 nm, respectively. The binary latex blend was prepared by mixing aqueous dispersions of Latex A and Latex B so that the final ratio in the blend was 1 : 1. After mixing with a magnetic stirrer for 20 min, a drop ($V \sim$ 100 μL) of the latex blend dispersion was cast on a freshly cleaved mica substrate ($\sim 1 \times 1$ cm^2 area). The film thickness was not determined, but it is expected to be in the range of several hundreds of micrometers. The samples were then dried in a desiccator under ambient conditions (25°C ± 2°C, 35% ± 3% RH) for 2 days (i.e., as-dried film) or annealed in an oven at 120°C (i.e., annealed film) for 60 min prior to analysis.

Scanning probe microscopy (SPM)

A Nanoscope IIIa (Digital Instruments Veeco Metrology Group, Santa Barbara, CA) SPM equipped with a MultiMode™ High Temperature Heater was used for thermal analysis and imaging of the sample surfaces. A specialized AS-130VT scanner including a resistive type heater, a thermocouple for sample temperature measurement, and water-fluid cooling protecting the piezoscanner elements from overheating was used. Uncoated 0.01–0.025 Ω cm Antimony (n) doped silicon probes supplied by the manufacturer (Veeco Instruments) were used for thermal analysis and imaging. Both the sample and the cantilever (probe) can be heated, simultaneously or separately, from ambient temperature up to 250°C. Here, only the probe was heated, that is, the sample was heated by the probe (heating-by-the-probe method).[51] The probe was installed in a special probe holder that allows for cantilever oscillation and probe heating, gas purging, and external temperature sensor access. Automatic tip-engage was initiated to bring the oscillating SPM tip into intermittent contact with the surface. After engaging the surface, the probe was retracted from the surface with a stepper motor to a fixed distance for thermal analysis. To estimate the distance corresponding to one step, the tip was re-engaged from which the distance to contact could be read. Repeated re-engagement gave as a result 5.2 ± 0.3 μm for the lift height. Since the tip height is about 10–15 μm, the actual distance of the probe (cantilever) from the surface was about 15–20 μm. The temperature of the probe was adjusted by applying a voltage to the probe heater with the Nanoscope™ Heater controller. The voltage was increased at a constant rate of 0.2 V per 5 min ($\sim$ 0.5°C/min). The exact temperature of the probe was set by utilizing an empirically obtained polynomial temperature–voltage calibration function.[51] After increasing the temperature of the probe to a predetermined value, the system was let to stabilize for 5 min. After stabilization, the resonant frequency of the probe was determined by sweeping the frequency near the nominal resonant frequency of the probe and simultaneously detecting the maximum amplitude of the oscillation. The observed frequency shifts ($\Delta\omega$) with respect to the initial nominal resonant frequency were then plotted as a function of temperature of the probe (T_p). As a calibration of the system, a linear change of the cantilever resonance frequency as a function of probe temperature

was observed by using mica as a substrate over a temperature range of 30–120°C.

The microscope was placed on an active vibration isolation table (MOD-1*M* JRS Scientific Instruments, Switzerland), which was placed on a massive stone table to eliminate external vibrational noise.

All the images (512 × 512 pixels) were measured under ambient conditions (25°C ± 3°C, 35% ± 5% RH) without filtering. The free amplitude of the oscillating cantilever (off contact) was set to 70 ± 5 nm. The engage procedure caused a shift in the resonance frequency that was taken into account. The new resonance frequency for the tip in contact with the sample was determined and used as the operating frequency. A damping ratio (contact amplitude/free amplitude) of about 0.5–0.6 was used for imaging. Images taken before and after the SPM probe annealing can be considered to be captured at exactly the same spot (with a lateral accuracy of ± 1.0 μm).

The Scanning Probe Image Processor (Image Metrology, Denmark) software was used for the roughness analysis of the images. Roughness parameters[54,55] were calculated for 3 × 3 μm^2 topographic images. Before the roughness analysis, LMS polynomial plane fit (first order) was applied to the unprocessed images.

Differential scanning calorimetry (DSC)

DSC (Mettler Toledo Stare System DSC 821e Module) was used to determine the glass transitions of the samples. The latex samples were first heated from –20 to 200°C (''first heating run''), then cooled to –20°C (''first cooling run''), and finally heated a second time to 200°C (''second heating run''). The heating/cooling rate was 10°C/min. The weight of the samples was about 5 mg. A linear background subtraction was applied to the DSC curves before analysis. The thermal transition temperatures were determined using the midpoint approximation.

Environmental scanning electron microscopy (ESEM)

Environmental Scanning Electron Microscopy (FEI quanta 200) was used to capture images of the latex samples before and after SPM probe annealing. The images were captured in high vacuum using an ETD detector and an accelerating voltage of 10.0 kV and 400× and 3000× magnification.

RESULTS AND DISCUSSION

The quality factor response of the scanning probe on the heat treatment

The value of the quality factor of the probe (Q_p) was observed to increase monotonically between 50°C and 80°C for the as-dried latex blend film at the tip-sample distance $d_{t\text{-}s} \approx 5$ μm [Fig. 1(A)]. At temperatures higher than 100°C, Q_p was found to be quite unstable; this may be due to an increased instability of the driving piezo.[56] On the other hand, for the blend sample annealed in an oven at 120°C, the values of Q_p measured at the same tip-sample distance remained quite constant within the measured temperature range [Fig. 1(B)]. The latter behavior coincides with the results of a previous report, where the quality factor was found to remain constant during a heating experiment of single-component latex films.[51] These different results motivated us to take a closer look at the thermal behavior and especially the probe-sample distance dependence of the quality factor.

The ΔQ_p-$d_{t\text{-}s}$ curve [Fig. 1(C)] at room temperature for a typical cantilever (probe) shows that Q_p remains constant when $d_{t\text{-}s} > 12$ μm. For smaller separations, a fairly linear ($R = 0.99148$) dependence of Q_p on the probe-sample distance was observed that may be expressed by the following equation:

$$\Delta Q_p \approx (9.5 \pm 0.6) d_{t\text{-}s} \quad (1)$$

This relation may be characteristic of the particular probe used, and the same probe was therefore used for all the measurements.[57] The decrease in Q_p with decreasing separation is due to a damping air film which is developed when an oscillating probe comes within ~ 10 μm from the sample surface.[58]

The trend demonstrated in Figure 1(C) may be used to interpret the difference between the curves of Figure 1(A,B). The sample of Figure 1(B) appears to be dimensionally stable during heating, whereas the increase in Q_p between 50 and 80°C for the as-dried blend sample suggests that the sample experienced a contraction. According to eq. (1), the vertical contraction was equal to 8.5 ± 0.7 μm. The sample contraction was confirmed by the fact that, after the sample had cooled to room temperature, the engagement distance to bring the oscillating SPM tip into intermittent contact with the sample surface had increased from about 5 μm to about 16 μm. This also indicates that the contraction of the sample was irreversible. The increase in engagement distance was more than the estimated sample contraction, perhaps because part of the thermal contraction was beyond the range within which Q_p is sensitive to the probe-sample distance. The extent of the thickness change experienced by the blend film indicates that heat was transferred relatively deep into the bulk. In fact, the heat dissipated from the probe has been shown to penetrate several hundred micrometers into the sample.[53]

The reason for the significant contraction of the as-dried latex blend film, in contrast to the behavior of

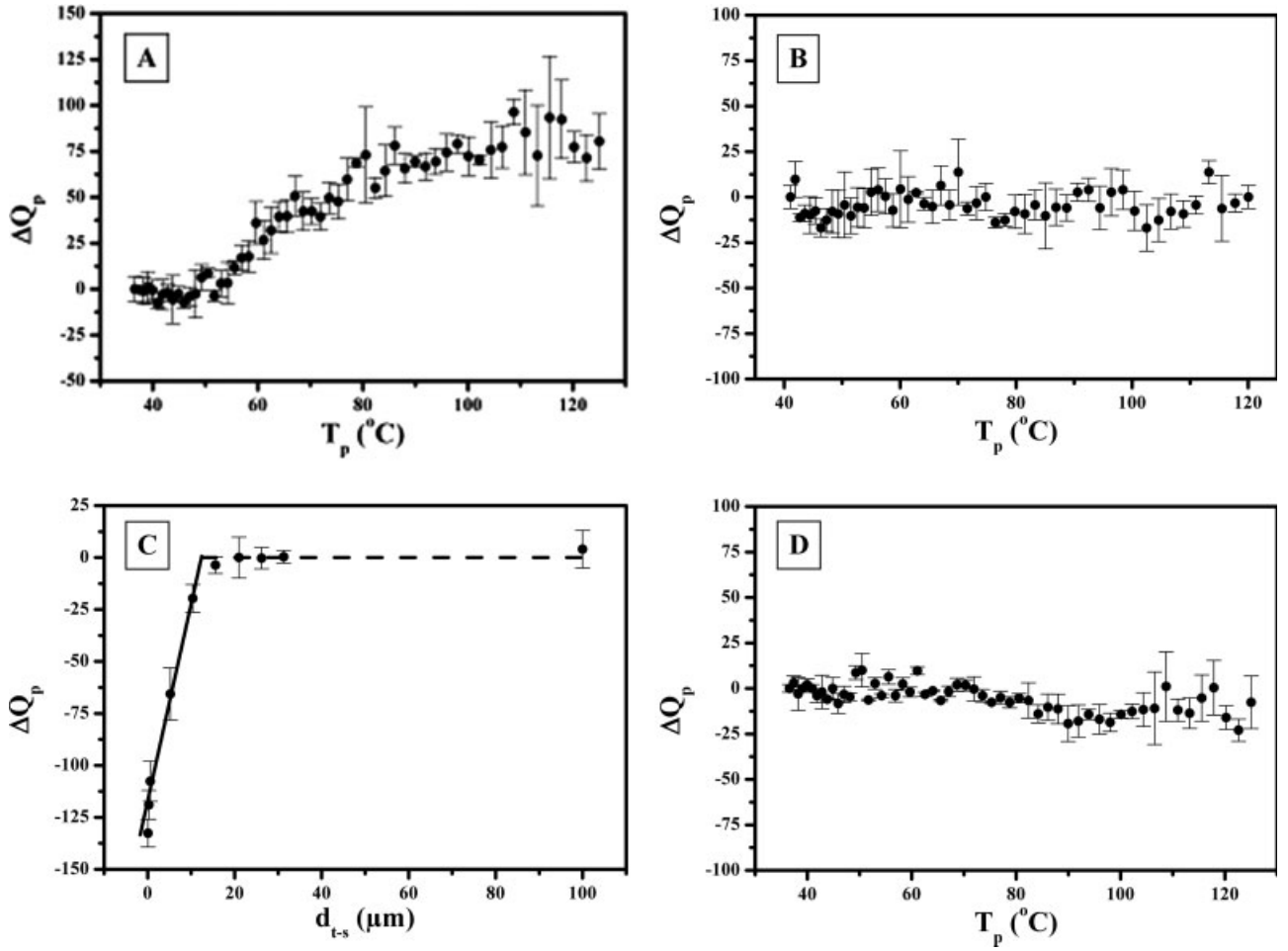

Figure 1 (A) ΔQ_p-T_p curve for the as-dried Latex A-Latex B (50 : 50 wt %) blend sample measured at $d_{t\text{-}s}$ = 5 μm. (B) ΔQ_p-T_p curve for the oven-annealed (120°C) blend sample measured at $d_{t\text{-}s}$ = 5 μm. (C) ΔQ_p-$d_{t\text{-}s}$ curve for the as-dried blend sample. The solid line shows a linear fit to the data points and the dashed line shows the constant region with no distance dependence. (D) ΔQ_p-T_p curve for the as-dried blend sample measured at $d_{t\text{-}s}$ = 30 μm.

the single-component films and the annealed blend sample, is not obvious. Water evaporation and a nonuniform surfactant concentration have however been shown to result in a contraction (thinning) of a drying latex film.[59]

The onset of the contraction seen in the ΔQ_p-T_p curve [Fig. 1(A)] coincides with the T_g value (53°C) determined by DSC, as well as with the melt onset temperature (50°C) measured by TMA for Latex A (low-T_g component).[52] This strongly suggests that the observed dimensional changes are related mainly to the onset of film formation of the low-T_g component in the blend film.

Since the contraction of the as-dried blend sample might influence the $\Delta\omega$-T_p curves, the tip-sample distance used for detecting thermal transitions in the as-dried blend sample was increased from 5 μm [linear region, Fig. 1(C)] to 30 μm (constant region). Indeed, the Q_p value remained constant when measurements were made at $d_{t\text{-}s}$ = 30 μm [Fig. 1(D)]; this indicates that ΔQ_p was insensitive to the dimensional changes. For the annealed blend sample, however, the tip-sample distance for the $\Delta\omega$-T_p measurements was kept at 5 μm.

The frequency response of the scanning probe on the heat treatment

Figure 2 shows the $\Delta\omega$-T_p curves for the as-dried (2A) and oven-annealed (2B) samples. Only one transition point is visible in each curve. The T_c values are practically the same for both samples, showing that the curing conditions had a negligible effect on the thermal properties of the blend. This is consistent with the results shown previously for bimodal 1 : 1 blends[2] and for single-component films of the same latices.[51] Evaporation of water from the latex films has been shown to contribute to the slope values and to the magnitude of the transition.[51] Systems with a higher moisture content exhibit an increase in the evaporation of water around the transition regime. This leads to higher evaporative cooling of the

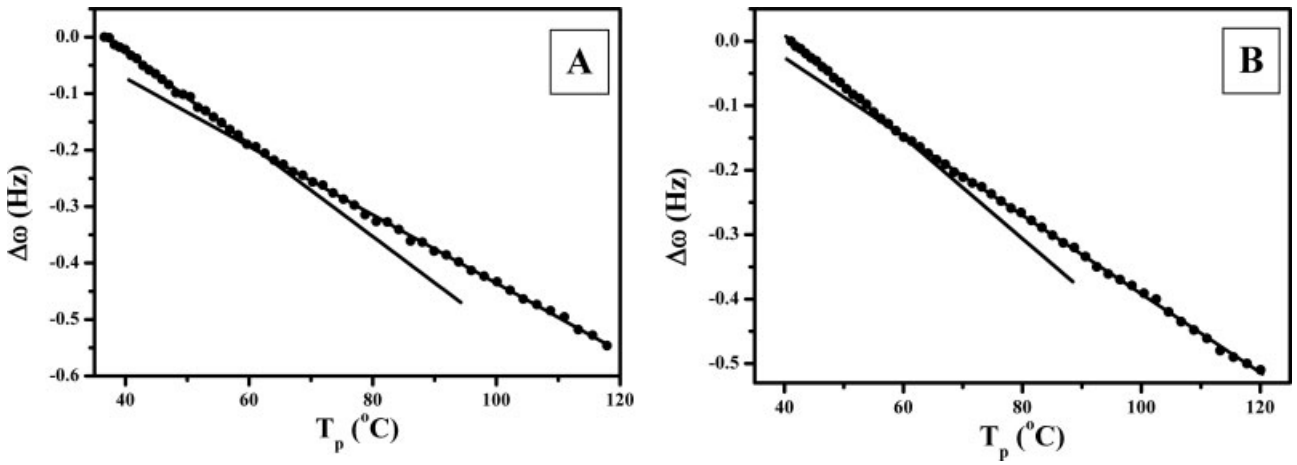

Figure 2 $\Delta\omega$-T_p -curves for (A) the as-dried Latex A-Latex B (50 : 50 wt %) blend sample and (B) the oven-annealed (120°C) blend sample. The solid lines in the curves show a linear fit to the data points. The intersection points indicate the critical transition point T_c.

probe and thus to a wider transition regime and a more distinct deviation from linearity in the $\Delta\omega$-T_p curve. The transition regime is evident only as a kink in a more moisture-free system. Both the pure and the blend films were analyzed at the center of the film.[51] The absence of any relatively broad transition region around T_c indicates that evaporation of bulk water in the as-dried blend film had proceeded further than in either of the pure Latex A and Latex B films. One reason for this may be a more porous structure of the as-dried blend film that facilitates evaporation of bulk water from the system. The ESEM micrographs of the surface of the as-dried Latex A film [Fig. 3(A)] and the Latex A-Latex B (50 : 50 wt %) blend film [Fig. 3(B)] indeed suggest that the blend system has a more porous structure.

The DSC thermograms obtained for the blend samples during the first and second heating runs are depicted in Figure 4(A,B). The following T_g values were obtained from the DSC curves: as-dried sample, first run: 57 and 83°C; second run: 60°C; sample oven-annealed at 120°C, first run: 50 and 75°C; second run: 62°C. The T_c values obtained from the $\Delta\omega$-T_p curves agree with those obtained from the second run DSC thermograms. However, T_c of 60°C does not match the T_c value of either of the pure Latex A (T_c = 49°C) or Latex B ($T_c \approx$ 80°C) components.[51,52] Actually, the T_c value for the blend is close to the average (64°C) of the T_c values of the pure components, considering a 1 : 1 mixture. Whether the film formation process is dominated by Latex A cannot be unambiguously concluded, but coincidently the minimum film formation temperature (MFFT) of Latex A (low-T_g component) having previously been estimated to be 65°C is quite close to the observed transition.[52]

Both the heating-by-the-probe SPM method and DSC define the glass transition as the temperature at

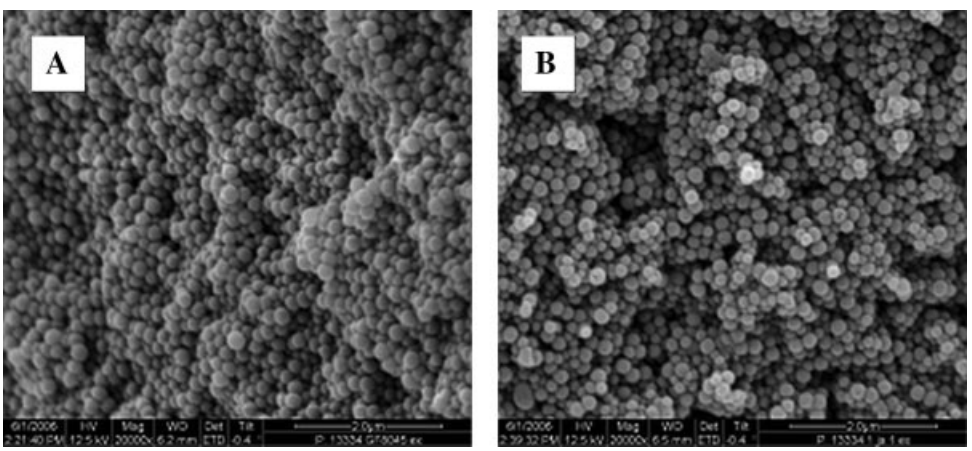

Figure 3 ESEM micrographs of a surface of (A) Latex A and (B) a Latex A-Latex B (50 : 50 wt %) blend. The scale bar is 2 μm.

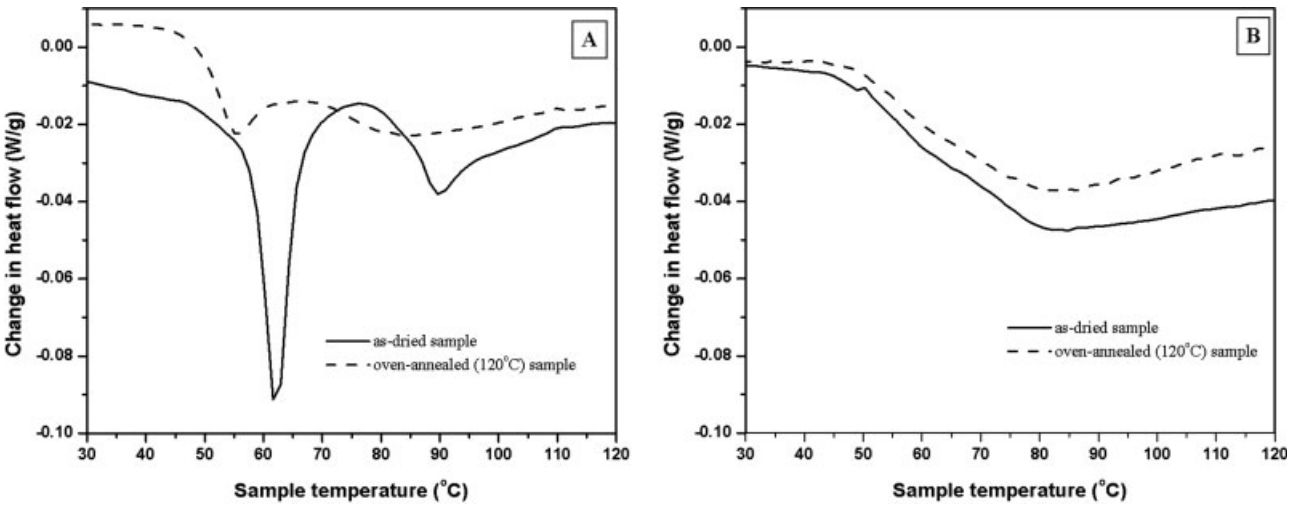

Figure 4 DSC thermograms of as-dried (solid line) and oven-annealed (dashed line) blend samples; (A) first run curves and (B) second run curves.

which there is a change in heat capacity as the sample transforms from a glassy to a rubbery state. However, relatively high heating rates have a tendency to introduce a nonreversible (kinetic) component in the DSC thermogram due to a volume relaxation in the system.[60,61] This is seen as a steep endothermic peak around the respective transition, as seen for example in Figure 4(A). The nonreversible phenomenon usually dominates over the reversible heat capacity change at the glass transition, making the separation of the former from the latter very difficult. Here, the heating rate in the DSC measurements was 10°C/min, whereas a heating rate of about 0.2°C/min was used in the heating-by-the-probe approach. The very slow heating rate is expected to significantly decrease the contribution of the volume relaxation. Endothermic volume relaxation peaks are clearly present in the first run DSC thermogram of the as-dried blend sample [Fig. 4(A)]. The endothermic peaks are also present in the first run thermogram of the oven-annealed blend sample, but with a much reduced intensity [Fig. 4(A)]. On the other hand, they are absent in the second run thermograms of both the samples [Fig. 4(B)]. Thus the two separate transitions seen in the first run thermogram [Fig. 4(A)] cannot be attributed solely to the change in heat capacity (heat flow) in the system but also have a strong volumetric relaxation contribution. This explains the discrepancy between the DSC (first run) and the $\Delta\omega$-T_p results and supports the conclusion drawn earlier that the change in the slope of the $\Delta\omega$-T_p curve is related purely to the change in heat capacity of the sample.[51]

Table I lists the slopes and their respective ratios for $\Delta\omega$-T_p curves before (S_1) and after (S_2) the transition (kink) point (T_c) for the as-dried and oven-annealed samples. In both cases, the slope is less above T_c and the ratio S_1/S_2 is approximately the same, despite the different thermal histories of the samples. In absolute terms, the change in slope of the $\Delta\omega$-T_p curves is generally small, due to the local nature of the measurement[51] and due to the fact that change in heat capacity at a glass transition is known to be very small.[26] The decrease in the slope after the transition, that is, the increase in the heat capacity, is consistent with previous results.[51] Furthermore, the negligible effect of the annealing conditions on the S_1/S_2 ratio has been demonstrated earlier.[51] The lower S_1/S_2 values of the pure latex components (1.16 for Latex A and 1.06 for Latex B)[51] than for the blend (Table I) indicate that the blend film exhibits the largest change in heat capacity at the transition. On the other hand, the change in heat capacity of Latex B (high-T_g component) is very small. The absence of the transition in the DSC second run curve [Fig. 4(B)] agrees with this result.

Heat-induced topography changes in the latex blend films

As-dried blend film

Figure 5(A) shows a typical high resolution (3 × 3 μm^2) SPM topography image of an as-dried blend film captured before any heat treatment. The

TABLE I
Values Taken From the $\Delta\omega$-T_p -Curves for the As-Dried and Oven-Annealed (120 °C) Latex A–Latex B (50 : 50 wt %) Blend Samples

Sample	S_1 (Hz/°C)	S_2 (Hz/°C)	S_1/S_2	T_c (°C)
As-dried	−8.2 ± 0.1	−6.1 ± 0.1	1.34	62°C
Annealed (120 °C)	−7.9 ± 0.1	−6.1 ± 0.1	1.30	60°C

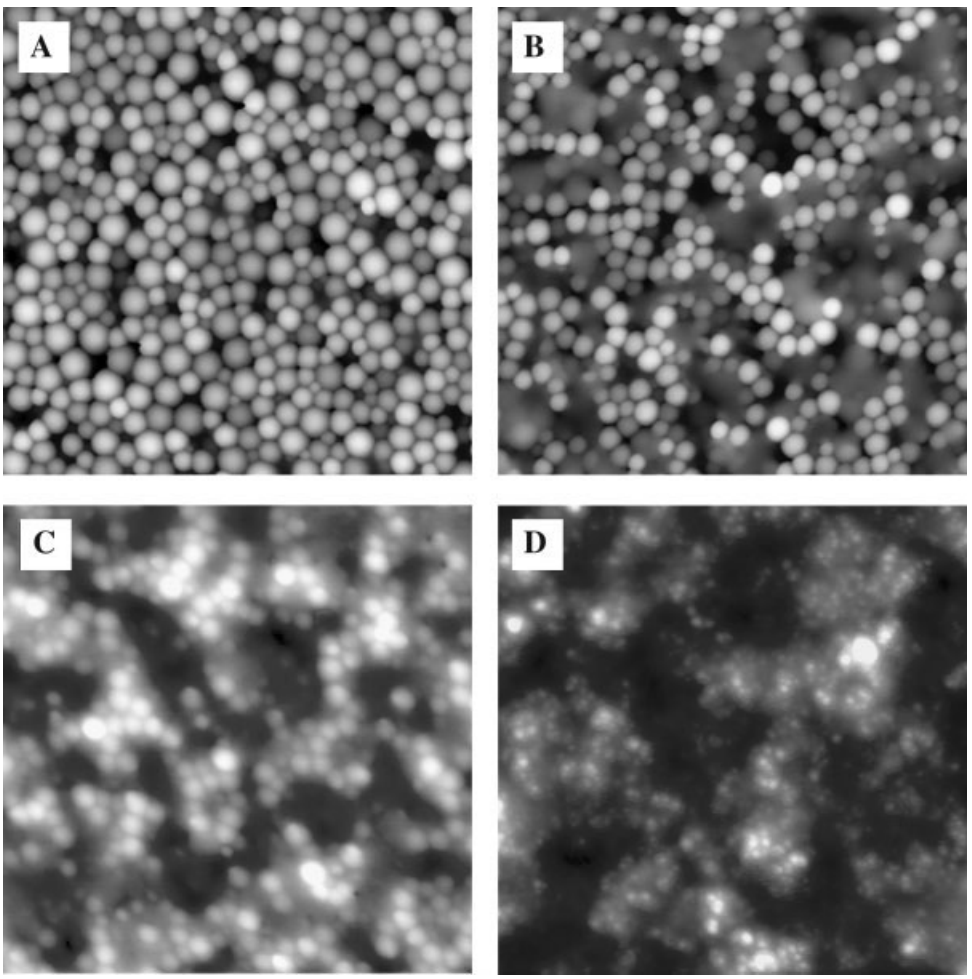

Figure 5 Typical SPM topography images of the as-dried Latex A-Latex B (50 : 50 wt %) blend film (A) before the thermal treatment by SPM probe, (B) after heating by the probe at T_p = 70°C, and (C) after heating by the probe at T_p = 120°C. (D) A typical SPM topography image of the oven-annealed (120°C) blend film before thermal treatment by SPM probe. The image size is 3 × 3 μm^2 and the height scales are (a) 200 nm, (b) 200 nm, (c) 50 nm, and (d) 60 nm.

particles visible can be divided into two groups according to the radius of curvature of individual particles: 108 ± 10 nm and 70 ± 12 nm. The values correspond well to the average diameter of the Latex A and Latex B components measured in the emulsions. In addition, the average particle-particle spacing (208 ± 8 nm for larger and 148 ± 8 nm for smaller particles) between neighboring particles of similar sizes and the corrugation height values (200 nm for the larger and 170 nm for the smaller particles) for individual particles measured next to the void areas were consistent with the dimensions of the pure components.

Particles of different sizes are fairly uniformly distributed on the surface [Fig. 5(A)] and are not clearly phase-separated, confirming that Latex A and Latex B particles are at least partially miscible. However, the abundant presence of relatively large void areas in the image suggests that the particles are somewhat clustered. This may be due to water evaporation.[11,17] The particles at the surface of the blend film appear to be slightly more clustered than what was previously observed for the films cast from single-component dispersions.[51] This is also seen in the ESEM images (Fig. 3). The 10-point height value (S_z ± S_q, using RMS roughness as standard deviation) of 291 ± 32.7 nm obtained from Figure 5(A) is clearly greater than the height expected for a monolayer, indicating that the two topmost layers of particles are not complete monolayers.

The particles in the blend have suffered negligible deformation due to drying at room temperature and have retained their spherical shape, which indicates that the capillary forces acting on the particles during the evaporation of water have not been sufficient to distort the latex particles.[11,17] One reason for the retained particle shape is probably that the alkyl diphenylene oxide sulfonate surfactant lowers the particle–water interface tension.[62,63] The degree of crosslinking of the polymers (the exact value is

unknown) and the loosely packed (porous) film structure probably contribute to the ability of the particles to resist deformation during film drying.[11,17] Furthermore, no flattening of the film had yet occurred as expected since the film was dried well below the T_g of both components in the mixture.[64–67] It has been shown previously that the surface and bulk morphologies of phase-separated soft/hard latex blends change progressively during thermal annealing. The surface of the film was changed from a particulate to a continuous phase morphology when the annealing temperature exceeded the T_g of the particles.[2]

As-dried blend film annealed with the SPM probe

Figure 5(B) shows a typical SPM topograph of a blend film captured after the sample had been heated by the probe to 70°C at a heating rate of about 0.2°C/min and then cooled to room temperature. The heating thus exceeded the T_g and MFFT of the low-T_g component (Latex A). In this case, the surface consisted of unevenly distributed spherical particles coexisting with another, relatively flat phase. The average radius of curvature of the particles was 83 ± 8 and the $d_{p\text{-}p}$ value between neighboring particles was 140 ± 36 nm. These values are comparable with the values obtained for Latex B particles in the as-dried blend film. It is thus evident that the flat phase corresponds to film-formed Latex A (soft phase). The surface area ratio of the flat and particle phases is unity which agrees with the 1 : 1 ratio of Latex A to Latex B in the blend. A small number of voids are discernible near the clusters of Latex B particles. The typical height of a particle next to a void was 173 nm ($S_z \pm S_q$ = 208 ± 31.3 nm), which agrees well with the dimensions of nondeformed Latex B particles. This is consistent with previously reported results that the spherical shape of hard particles is retained when the annealing temperate is below the T_g of the hard component.[3,23] No voids were observed on the surface of the films made from pure Latex A and Latex B dispersions.[51] Although the addition of nonfilm-forming (hard) particles to a film-forming latex is known to generate voids in the film.[15,19,68] Such voids are created because hard particles cannot deform to fill the interstices after moisture evaporation. If the mobility of soft latex polymer chains is sufficiently high, the film-forming ability in a binary blend is controlled by the number of contacts between hard particles.[15] The maximum weight fraction of the high T_g emulsion polymer for transparent and void-free films has been reported to be 0.55.[15] Packing in a soft/hard blend is a function of the particle size ratio. When the size ratio is slightly over 1.0 (as in the present case), the soft components are known to act as a continuous phase whereas hard particles disperse unevenly and voids are formed.[3]

In the flat phase, the Latex A particles have lost their topographical identity, including their curvature at the latex–air interface [Fig. 5(B)]. Flattening of particles has been known to occur in non-crosslinked polymers when the temperature is maintained above their T_g.[64–67] The main driving force for flattening has been identified to be the polymer–air surface energy.[64–67] Although Latex A polymer is crosslinked, the degree of crosslinking must be sufficiently low for the flattening to occur. In other words, the polymer–air surface energy must be stronger than the increase in internal viscosity due to the reduced chain mobility that resists the flattening process.

Another phenomenon that may occur simultaneously with flattening during film formation is interparticle migration of the polymer chains (diffusion across the particle boundaries).[11,17] It has previously been shown that this takes place in single-component latex films,[51] but probably only to a limited extent, since crosslinking and the presence of surfactants are known to hinder interparticle diffusion.[11,17] However, in immiscible blends, unfavorable thermodynamics will lead to very limited diffusion across the particle interfaces. Thus, it is believed that no significant interdiffusion (autohesion) occurred in the blend film.

Figure 5(C) shows a typical SPM topographic image for the blend sample captured after the sample had been heated by the probe to T_p = 120°C, that is, well above the T_g and MFFT of both components in the blend. The topograph shows that particles still remain on the surface, and the clustering of the particles indicates partial phase separation. The average radius of curvature of the particles was considerably larger (344 ± 43 nm) than that of Latex B particles in Figure 5(A,B), indicating some flattening and deformation of Latex B particles. In fact, the very small average height (12 nm) of Latex B particles suggests that the deformation is quite extensive and that film formation is close to its final stage. The spherical form of the latex particles is maintained to minimize the surface free energy until the film is completely flattened.[64–67] Despite the particle deformation, the distance between neighboring particles ($d_{p\text{-}p}$ = 132 ± 30 nm) is approximately the same as the value obtained for the as-dried film [Fig. 5(A)], which also agrees with the previous model presented for the flattening of a latex film.[64–67] Furthermore, void areas are practically absent in the image [Fig. 5(C)], which is also indicated by the significantly lower $S_z \pm S_q$ value (57.5 ± 10.0 nm) than that for Figure 5(B). It can hence be concluded that both latices form a film when annealed at a sufficiently high temperature.

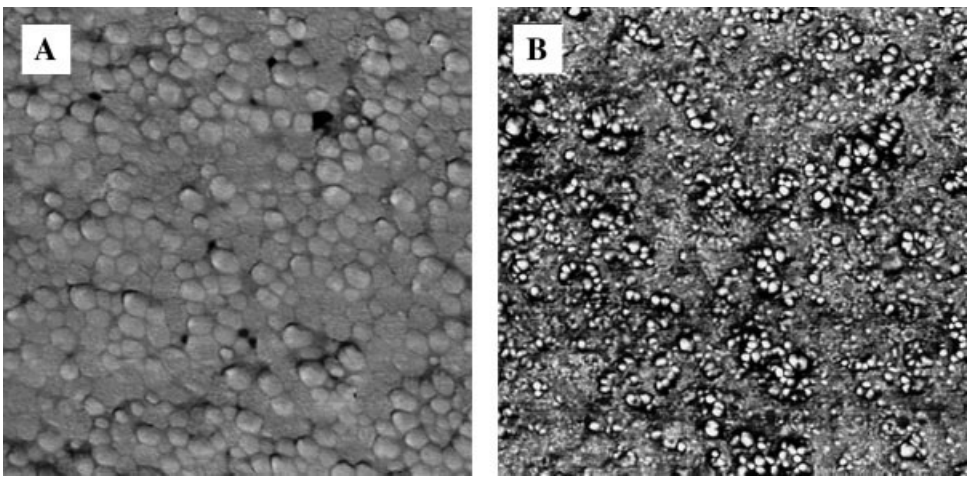

Figure 6 (A) A typical SPM phase image of (A) an as-dried Latex A-Latex B (50 : 50 wt %) blend film after the thermal treatment by SPM probe up to T_p = 120°C. (B) A typical SPM phase image of the oven-annealed (120°C) Latex A-Latex B (50 : 50 wt %) blend film before any thermal treatment by an SPM probe. The image size is 3 × 3 μm^2 and the dark-light contrast scale 30 degrees.

Oven-annealed blend film

Figure 5(D) shows a typical SPM topographic image of the Latex A-Latex B (50 : 50 wt %) blend sample annealed in an oven at 120°C for 60 min. The image was captured before any probe heating was applied to the sample. The surface appears to be devoid of structure and includes few particles of irregular shape. The $S_z \pm S_q$ value of 72 ± 8 nm is slightly higher than that of the probe-heated sample [Fig. 5(C)]. It is obvious that the oven-annealing and the SPM probe annealing have different effects on the morphology of the blend film. There were no significant changes in surface morphology when the oven-annealed sample was heat-treated with an SPM probe (data not shown). This is consistent with previous results obtained for the films made from single-component latex dispersions.[51]

The small exudates seen in Figure 5(D) are believed to be surfactant or other components in the latex serum that have migrated and segregated onto the latex blend surface during oven-annealing. However, no surface chemical analysis was carried out to confirm this claim. The migration has been reported to occur mainly due to a water flux driving low molecular weight species to the film–air interface.[69] Additional information about the surface structure was obtained from the SPM phase contrast images (Fig. 6). The phase image for the as-dried blend sample [Fig. 6(A)] appears to be very homogeneous, with the only contrast corresponding to structural grain boundaries. The phase image for the oven-annealed sample [Fig. 6(B)] is much more heterogeneous. The exudates appear as light areas, that is, the energy dissipation and thereby the phase shift is larger than that measured for the surrounding surface.[70,71] This indicates that the particles seen in Figure 5(C,D) have mechano-chemical properties different from the surrounding phase.

The effects of different annealing methods on the presence or absence of exudates on the surface of latex samples has been previously reported for films made from single-component dispersions.[51] One explanation given for the difference was that SPM probe annealing seals the surface and thereby prevents migration from the bulk. It has also been reported that migration of surfactants onto the film–air surface in the soft/hard latex blend systems occurred only when the annealing temperature was higher than the T_g of the hard component.[69] The migrating surfactant molecules absorbed on or embedded in the hard particles are released only when coalescence of the particles is initiated. This may explain the absence of exudates on the surface of the blend film annealed at T_p = 70°C [Fig. 5(B)], even though the surface was obviously not sealed.

CONCLUSIONS

The results demonstrate that SPM is well suited for the study of thermal properties and film formation of latex films. Thermal transitions associated with changes in heat capacity and dimensional stability in latex blend systems were detected. The results show the high sensitivity of SPM to detect thermal transitions even though glass transitions are normally associated with a very small change in heat capacity.[26] The glass transition temperatures determined by SPM were in agreement with those measured by DSC data. These methods may, however, also be regarded as being complementary; DSC measures bulk properties whereas SPM is a more surface-sensitive method and facilitates dimensional

stability studies. The slow heating rate of the SPM system eliminates the contribution of volumetric changes involved in DSC measurements around T_g.

The glass transition data obtained by SPM yielded new information about the nature of the transition, that is, differences in water evaporation in different systems, the strength of the transition being characteristic of the latex, and the response of different components in a blend film to heating. In fact, transitions of individual components in a blend system could be followed, yielding useful information about the compatibility of the components in a blend film.

The type of annealing was one variable studied. It was found that thermal annealing in an oven did not influence the transition associated with the change in heat capacity, but it did influence the dimensional stability of the film. The thermal transition temperatures observed in the $\Delta\omega$-T_p and ΔQ_p-T_p curves were also found to coincide with the MFFT and onset temperature of vertical contraction.

Further information on the compatibility of film components was obtained from the topographical studies of the films. The components were identified by their dimensions, and a description of the surface topography in terms of roughness parameters enabled the film formation from a particulate to a continuous film to be followed in detail. Such an analysis can be utilized to tune the composition of a blend film to obtain improved performance. Detailed surface chemical analysis would provide further information about the local composition of the films.

Omnova Solutions (USA) is thanked for providing samples. Dr. Anthony Bristow is thanked for the linguistic revision of the manuscript.

References

1. Utracki, L. A. Polymer Blends Handbook; Kluwer Academic Publishers: Dordrecht, 2002; Vol. 1–2.
2. Colombini, D.; Hassander, H.; Karlsson, O. J.; Maurer, F. H. J. J Polym Sci Part B: Polym Phys 2005, 43, 2289.
3. Colombini, D.; Hassander, H.; Karlsson, O. J.; Maurer, F. H. J. Macromolecules 2004, 43, 6865.
4. Spiro, J. G.; Farinha, J. P. S.; Winnik, M. A. Macromolecules 2003, 36, 7791.
5. Tang, J.; Daniels, E. S.; Dimonie, V. L.; Vratsanos, M. S.; Klein, A.; El-Aasser, M. S. J Appl Polym Sci 2002, 86, 2788.
6. Dinelli, F.; Buenviaje, C.; Overney, R. M. Thin Sol Films 2001, 396, 138.
7. Robeson, L. M.; Berner, R. A. J Polym Sci Part B: Polym Phys 2001, 39, 1093.
8. Agarwal, N.; Farris, R. J. Polym Eng Sci 2000, 40, 376.
9. Robeson, L. M.; Vratsanos, M. S. Macromol Symp 2000, 155, 117.
10. Tzitzinou, A.; Keddie, J. L.; Geurts, J. M.; Peters, A. C. I. A.; Satguru, R. Macromolecules 2000, 33, 2695.
11. Steward, P. A.; Hearn, J.; Wilkinson, M. C. Adv Colloid Interface Sci 2000, 86, 195.
12. Chevalier, Y.; Hidalgo, M.; Cavaillé, J.-Y.; Cabane, B. Macromolecules 1999, 32, 7887.
13. Feng, J.; Odrobina, E.; Winnik, M. A. Macromolecules 1998, 31, 5290.
14. Feng, J.; Winnik, M. A.; Siemiarczuk, A. J Polym Sci Part B: Polym Phys 1998, 36, 1115.
15. Lepizzera, S.; Lhommeau, C.; Dilger, G.; Pith, T.; Lambla, M. J Polym Sci Part B: Polym Phys 1997, 2093, 35.
16. Eckersley, S. T.; Bradley, B. J. J Coat Technol 1997, 69, 97.
17. Keddie, J. L. Mater Sci Eng 1997, R21, 101.
18. Peters, A. C. I. A.; Overbeek, G. C.; Buckmann, A. J. P.; Padget, J. C.; Annable, T. Prog Org Coat 1996, 29, 183.
19. Keddie, J. L.; Meredith, P.; Jones, R. A. L.; Donald, A. M. Langmuir 1996, 12, 3793.
20. Winnik, M. A.; Feng, J. J Coat Technol 1996, 68, 39.
21. Heuts, M. P. J.; le Febre, R. A.; van Hilst, J. L. M.; Overbeek, G. C. ACS Symp Ser 1996, 648, 271.
22. Patel, A. A.; Feng, J.; Winnik, M. A.; Vancso, G. J.; Dittman McBain, C. B. Polymer 1996, 37, 5577.
23. Feng, J.; Winnik, M. A.; Shivers, R. R.; Clubb, B. Macromolecules 1995, 28, 7671.
24. Cavaillé, J. Y.; Vassoille, R.; Thollet, G.; Rios, L.; Pichot, C. Colloid Polym Sci 1991, 269, 248.
25. Brandrup, J.; Immergut, E. H.; Grulke, E. A. Polymer Handbook, 4th ed.; Wiley: New York, 1999.
26. Fischer, H. Macromolecules 2005, 38, 844.
27. Wang, C. Thermochim Acta 2004, 423, 89.
28. Tsukruk, V. V.; Gorbunov, V. V.; Fuchigami, N. Thermochim Acta 2003, 395, 151.
29. Lemieux, M.; Minko, S.; Usov, D.; Stamm, M.; Tsukruk, V. V. Langmuir 2003, 19, 6126.
30. Luzinov, I.; Julthongpiput, D.; Tsukruk, V. V. Polymer 2001, 42, 2267.
31. Hammiche, A.; Pollock, H. M. J Phys D: Appl Phys 2001, 34, R23.
32. Tsukruk, V. V.; Huang, Z. Polymer 2000, 41, 5541.
33. Hammiche, A.; Reading, M.; Pollock, H. P.; Song, M.; Hourston, D. J. Rev Sci Instrum 1996, 67, 4268.
34. Majumdar, A.; Carrejo, P. C.; Lai, J. Appl Phys Lett 1993, 62, 2501.
35. Majumdar, A. Annu Rev Mater Sci 1999, 29, 505.
36. Pearce, R.; Vancso, G. J. Macromolecules 1997, 30, 5843.
37. Hobbs, J. K.; McMaster, T. J.; Miles, M. J.; Barham, P. J. Polymer 1998, 39, 2437.
38. Godovsky, Y. K.; Papkov, V. S.; Magonov, S. N. Macromolecules 2001, 34, 976.
39. Schönherr, H.; Bailey, L. E.; Frank, C. W. Langmuir 2002, 18, 490.
40. Kajiyama, T.; Tanaka, K.; Takahara, A. Polymer 1998, 39, 4665.
41. Hammerschmidt, J.; Gladfelter, W.; Haugstadt, G. Macromolecules 1999, 32, 3360.
42. Tanaka, K.; Taura, A.; Ge, S.; Takahara, A.; K ajiyama, T. Macromolecules 1996, 29, 3040.
43. Sills, S.; Overney, R. M.; Chau, W.; Lee, V. Y.; Miller, R. D.; Frommer, J. J Chem Phys 2004, 120, 5334.
44. Ge, S.; Pu, Y.; Zhang, W.; Rafailovich, M.; Sokolov, J.; Buenviaje, C.; Buckmaster, R.; Overney, R. Phys Rev Lett 2000, 85, 2340.
45. Bliznyuk, V.; Assender, H.; Briggs, G. Macromolecules 2002, 35, 6613.
46. Oulevey, F.; Burnham, N.; Gremaud, G.; Kulik, A.; Pollock, H. M.; Hammiche, A.; Reading, M.; Song, M.; Hourston, D. Polymer 2000, 41, 3087.
47. Meincken, M.; Sanderson, R. D. S Afr J Sci 2004, 100, 256.
48. Meincken, M.; Balk, L. J.; Sanderson, R. D. Surf Interface Anal 2003, 35, 1034.
49. Meincken, M.; Graef, S.; Mueller-Nedebock, K.; Sanderson, R. D. Appl Phys A 2002, 74, 371.
50. Meincken, M.; Balk, L. J.; Sanderson, R. D. Macromol Mater Eng 2001, 286, 412.

51. Ihalainen, P.; Backfolk, K.; Sirviö, P.; Peltonen, J. J Appl Phys 2006, 101: 043505-1.
52. Backfolk, K.; Holmes, R.; Ihalainen, P.; Sirviö, P.; Triantafillopoulos, N.; Peltonen, J. Polym Test 2007, 26, 1031.
53. Backfolk, K.; Sirviö, P.; Ihalainen, P.; Peltonen, J.; Thermochim Acta 2008, 470, 27.
54. Dong, W. P.; Sullivan, P. J.; Stout, K. J. Wear 1994, 178, 29.
55. Dong, W. P.; Sullivan, P. J.; Stout, K. J. Wear 1994, 178, 45.
56. Prillman, S. G.; Kavanagh, A. M.; Scher, E. C.; Robertson, S. T.; Hwang, K. S.; Colvin, V. L. Rev Sci Instrum 1998, 69, 3246.
57. Yasumura, K. Y.; Stowe, T. D.; Chow, E. M.; Pfafman, T.; Kenny, T. W.; Stipe, B. C.; Rugar, D. J Microelectromech Syst 2000, 9, 117.
58. Digital Instrument, Inc., Nanoscope III, Control System User's Manual, 1996.
59. Gundabala, V. R.; Routh, A. F. J Colloid Interface Sci 2006, 303, 306.
60. Thomas, L. C. Am Lab 2001, 33, 26.
61. Pyda, M.; Wunderlich, B. Macromolecules 2005, 38, 10472.
62. Dimonie, V. L.; El-Asser, M. S.; Vanderhoff, J. W. Makromol Symp 1990, 35/36, 447.
63. Vanderhoff, J. W.; Dimonie, V. L.; El-Asser, M. S.; Settlemeyer, L. A. J Appl Polym Sci 1990, 41, 1549.
64. Pérez, E.; Lang, J. Langmuir 2000, 16, 1874.
65. Pérez, E.; Lang, J. Macromolecules 1999, 32, 1626.
66. Lin, F.; Meier, D. J. Langmuir 1996, 12, 2774.
67. Lin, F.; Meier, D. J. Langmuir 1995, 11, 2726.
68. Ho, C. C.; Khew, M. C.; Liew, Y. F. Surf Interface Anal 2001, 32, 133.
69. Zhao, Y.; Urban, M. W. Macromolecules 2000, 33, 2184.
70. Garcia, R.; Perez, R. Surf Sci Rep 2002, 47, 197.
71. Garcia, R.; Magerle, R.; Perez, R. Nat Mater 2007, 6, 405.